N-Nitrosotolazoline: Decomposition Studies of a Typical *N*-Nitrosoimidazoline

Richard N. Loeppky*,† and Jianzheng Shi

Department of Chemistry, University of Missouri, Columbia, Missouri 65211

Received September 6, 2007

N-Nitrosotolazoline (*N*-nitroso-2-benzylimidazoline), a *N*-nitrosated drug typical of *N*-nitrosoimidazolines, reacts readily with aqueous acid, nitrous acid, or *N*-acetylcysteine to produce highly electrophilic diazonium ions capable of alkylating cellular nucleophiles. The kinetics and mechanism of the acidic hydrolytic decomposition of *N*-nitrosotolazoline have been determined in mineral acids and buffers. The mechanism of decomposition in acidic buffer is proposed to involve the rapid reversible protonation of the imino nitrogen atom followed by slow general base-catalyzed addition of H_2O to the 2-carbon of the imidazoline ring to give a tetrahedral intermediate, which is also a α-hydroxynitrosamine. Rapid decomposition of this species gives rise to the diazonium from which the products are derived by nucleophilic attack, elimination, and rearrangement. The proposed mechanism is supported by the observations of general acid catalysis, a negligible deuterium solvent kinetic isotope effect (k_H/k_D = 1.15) and $\Delta S^{\ddagger} = -34$ eu. In phosphate buffer at 30 °C, the half-lives of *N*-nitrosotolazoline range from 5 min at pH 3.5 to 4 h at pH 6. The main reaction product of the hydrolytic decomposition is *N*-(2-hydroxyethyl)phenylacetamide. This and other products are consistent with the formation of a reactive diazonium ion intermediate. *N*-Nitrosotolazoline nitrosates 50 times more rapidly than tolazoline and results in a set of products derived from reactive diazonium ions but different from those produced from the hydrolytic decomposition of the substrate. *N*-Acetylcysteine increases the decomposition rate of *N*-nitrosotolazoline by 25 times at pH 7 and results in both *N*-denitrosation and induced decomposition to produce electrophiles. These data suggest that *N*-nitrosotolazoline shares the chemical properties of many known direct-acting mutagens and carcinogens.

Introduction

Tolazoline **1**, a nasal decongestant and antihypertensive agent, is structurally typical of a growing number of imidazoline-based drugs (*1*). These substances contain a 2-substituted imidazoline ring and are secondary amidines, which can generate *N*-nitrosoimidazolines upon nitrosation. In the previous publication, we showed that *N*-nitrosotolazoline **2**, and products derived from it, are produced from **1** under nitrosation conditions, which vary from those encountered endogenously in humans to those used purely for the purposes of laboratory investigation (*1*). Because *N*-nitrosotolazoline is representative of *N*-nitrosoimidazolines, which could be produced from the endogenous nitrosation of imidazoline-based drugs and other substances, we have investigated the chemical properties of **2** under several conditions that it is likely to encounter upon endogenous production. We report here on the kinetics and products of the acid-catalyzed hydrolysis of *N*-nitrosotolazoline, on its facile nitrosation, and on its denitrosation and other transformations resulting from its reaction with *N*-acetylcysteine, a model thiol. These studies have shown that the chemistry of *N*-nitrosotolazoline is not at all typical of nitrosamines but is more similar to *N*-nitrosoamides, *N*-nitrosoureas, and *N*-nitrosocarbamates, which are direct-acting mutagens and carcinogens.

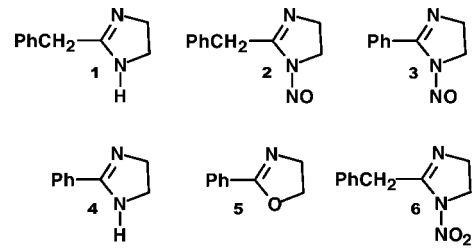

In addition to our prior work on amidine and imidazoline nitrosation (*2–4*), there are two important publications by Iley and co-workers that are relevant to the research being presented here. In the first study, the kinetics of the acid-catalyzed hydrolytic decomposition of several *N*-nitroso-2-arylimidazolines, most particularly *N*-nitroso-2-phenylimidazoline **3**, are reported (*5*). While we compare their kinetic data and conclusions with ours later in this paper, it is notable that **3** is reported to denitrosate to 2-phenylimidazoline **4** and also produce 2-phenyl-1,3-oxazoline **5** from the intramolecular trapping of a diazonium ion. These types of products are not significant ones arising from the acid-catalyzed decomposition of *N*-nitrosotolazoline. In the second study, the Iley group examined the acid-catalyzed decomposition of *N*-nitrotolazoline **6**, which arises from the reaction of tolazoline with N_2O_4 (*6*). The aqueous acid-induced decomposition of **2** or **6** results in the same major product, *N*-2-hydroxyethylphenylacetamide.

Experimental Procedures

Caution: *Most nitrosamines are potent carcinogens. Considerable care should be taken in their use so as to avert*

* To whom correspondence should be addressed. Tel: 425-493-1302. E-mail: LoeppkyR@Missouri.edu.

† Visiting Scholar, Department of Medicinal Chemistry, University of Washington, Seattle, Washington 98195.

10.1021/tx700318k CCC: $40.75
Published on Web 01/31/2008

exposure to humans and to avoid environmental contamination. We routinely perform all operations with these substances, except for dilute solutions thereof, in well-ventilated fume hoods. We rinse all nitrosamine-contaminated glassware with a solution of concentrated HBr in glacial acetic acid (1:1), which is effective in cleaving the NO group form the amine nitrogen atom. The action of this agent in aprotic solutions is also effective in nitrosamine destruction. Aqueous solutions are treated with either Ni(R) or Al in concentrated sodium hydroxide. This process may produce hydrazines.

General. The instrumentation and reagents are the same as noted in the previous paper (*1*).

Identification of Products from the Decomposition of *N*-Nitrosotolazoline 2. *N*-Nitrosotolazoline (**2**, 200 mg, 1.06 mmol) was dissolved in 1.0 mL of acetonitrile. To this solution, 20 mL of 0.1 M HCl was added. The mixture was stirred at room temperature for 12 h and then extracted with CH_2Cl_2 (15 mL × 3). The combined organic layers were washed with saturated salt solution, dried over Na_2SO_4, and concentrated. The residue was purified by flash chromatography using hexane/EtOAc (from 4:1 to pure EtOAc) as an eluent. Three products were obtained as white solids.

***N*-(2-Hydroxyethyl)phenylacetamide 7 (*6*).** Yield, 70%; mp 59–60 °C. ^{1}H NMR: δ 7.27 (m, 5 H), 6.57 (b, 1 H), 3.76 (b, 1 H), 3.56 (t, $J = 5.3$, Hz, 2 H), 3.50 (s, 2H), 3.29 (t, $J = 5.3$ Hz, 2 H). ^{13}C NMR: δ 172.4, 134.7, 129.2, 128.7, 127.1, 61.4, 43.3, 42.4. EIMS (relative intensity): 179 ($M^{\bullet+}$ 8), 161(12), 136 (30), 91 (100).

***N*-(1-Hydroxyethyl)phenylacetamide 12.** Yield, 13%; mp 99–100 °C. ^{1}H NMR: δ 7.34 (m, 5 H), 5.97 (b, 1 H), 5.46 (m, $J = 6.0$ Hz, 1 H), 3.83 (b, 1 H), 3.57 (s, 2 H), 1.26 (d, $J = 6.0$ Hz, 3 H). ^{13}C NMR: δ 172.3, 134.1, 129.4, 129.1, 127.5, 71.7, 43.6, 20.8. IR (KBr): 3268 (s), 3064, 1654 (s), 1548 (s), 1135, 1078, 918 cm^{-1}. HRMS calcd for $C_{10}H_{13}NO_2 + Na^+$, 202.0844; found, 202.0839. (See the Supporting Information for the X-ray crystal structure.) This compound was also prepared for comparison as follows: A mixture of phenylacetamide (242 mg, 2 mmol), acetaldehyde (114 mg, 2.6 mmol), and K_2CO_3 (27.6 mg, 0.2 mmol) in 2 mL of toluene was stirred for 6 days. TLC showed no difference between 2 and 6 days. After purification by flash column (4:1, v/v EtOAc and hexane), the product was isolated as a white solid (85 mg, 25%). Its properties were identical to those of the substance isolated from the decomposition mixture.

***N*-Vinylphenylacetamide 10 (*7*).** Yield, 2–3%; mp 81–82 °C. ^{1}H NMR: δ 7.38 (m, 5 H), 6.96 (dd, $J = 15.6$, 8.2 Hz, 1 H), 6.93 (b, 1 H), 4.48 (dd, $J = 15.6$, 2.4 Hz, 1 H), 4.37 (dd, $J = 8.2$, 2.4 Hz, 1 H), 3.64 (s, 2 H). ^{13}C NMR: δ 168.3, 133.9, 129.5, 129.2, 128.4, 127.7, 95.7, 43.6. IR (KBr): 3231, 3137, 3027, 1634 (s), 1511, 1262, 1192 cm^{-1}.

2-Aminoethyl Phenylacetate 8. In a separate experiment, the acidic decomposition mixture was extracted with several portions of ethyl acetate to remove the compounds described above. The aqueous fraction was concentrated to 2 mL under vacuum. Acetone was slowly added to this solution until the formation of a white precipitate was complete. This compound (*8*) was the hydrochloride of **8** (18% yield). ^{1}H NMR (in DMSO-d_6): δ 8.33 (b, 3 H), 7.28 (m, 5 H), 4.24 (t, $J = 5.2$ Hz, 2 H), 3.74 (s, 2 H), 3.07 (t, $J = 5.2$ Hz, 2 H). ^{13}C NMR: δ 171.1, 134.1, 129.5, 128.3, 126.8, 60.7, 40.0, 37.7.

LC-MS/MS of Reaction Mixture. In a separate set of experiments when the decomposition was conducted either as described above or in aqueous acetic acid, the reaction mixture was subjected to LC-MS/MS using a Zorbak SB C-8 4.6 mm × 250 mm column employing 0.1% formic acid (A) and acetonitrile (B) as eluents using a 40 min linear gradient of 90% A to 90% at a flow rate of 1 mL/min. MS/MS and standards were then utilized to identify compounds **1**, **2**, and **7**−**13**.

Kinetics of *N*-Nitrosotolazoline Decomposition. The kinetics of the decomposition of *N*-nitrosotolazoline **2** were determined on a HP diode array UV–visible spectrometer, using various acids as discussed in the Results and Discussion section. All reactants were brought to the desired temperature in a constant temperature bath prior to mixing. Transformations were conducted at the same temperature. In a typical experiment, *N*-nitrosotolazoline solution (2 μL, 8 mM) in CH_3OH was transferred to a cuvette with a syringe and diluted with a perchloric acid solution containing 1 M $NaClO_4$ to maintain ionic strength to an initial concentration of 80 μM. The kinetic decay was monitored by the UV absorbance changes at 259 nm. The observed rate constant k_{obs} was obtained by linear regression of ln ($A_t - A_\infty$) vs time.

Reaction of *N*-Acetylcysteine 33 and 2. A series of phosphate buffers (0.5 M) with different concentrations of *N*-acetylcysteine **33** (0, 0.01, 0.1, and 0.5 M, respectively) were made, and the pH was adjusted to 4.0 or 5.0. Aliquots of solutions of **2** (in CH_3CN) were added to these buffers to bring the concentration to 2.7 mM. The sample vials maintained at room temperature (≈23 °C) were placed in an HPLC autosampler holder and injected onto the HPLC every 25 min. The substrate and product concentrations at each time were determined from calibration curves of authentic samples. HPLC comparisons of decomposition mixtures with or without **33** gave the retention volumes of the new products in the reactions with **33**. *N*-Nitrosotolazoline **2** and **33** (0.5 M) were allowed to react at pH 5 for 77 min. The new products were isolated by preparative HPLC. Under these conditions, the yields were as follows: **7**, 36.5%; tolazoline **1**, 13.2%; unreacted *N*-nitrosotolazoline **2**, 7%; *S*-phenylacetyl-*N*-acetylcysteine **34**, 14%; and (2-phenylacetylamino)ethyl *N*-acetylcysteine **35**, 5%.

***S*-Phenylacetyl-*N*-acetylcysteine 34.** ^{1}H NMR ($CDCl_3$): δ 7.9 (br s, 1 H), 7.28 (m, 5 H), 6.46 (d, 1 H), 4.67 (dd, 1H), 3.85 (s 2 H), 3.35 (m, 2 H), 1.90 (s, 3 H). ^{13}C NMR: δ 198.02, 172.18, 171.85, 133.01, 129.46, 128.78, 127.64, 52.76, 50.30, 30.30, 22.55. HRMS calcd for $C_{13}H_{15}NO_4S + H^+$, 282.0800; found, 282.0800.

2-Phenylacetylaminoethyl *N*-Acetylcysteine 35. *N*-Phenylacetylaziridine **36** was prepared by the procedure reported by Boggs et al. (*9*). For **36**: ^{1}H NMR ($CDCl_3$): δ 7.22 (m, 5 H), 3.67 (s, 2 H), 2.10 (s, 4 H). ^{13}C NMR: δ 183.3, 134.4, 129.2, 128.5, 126.9, 44.0, 24.2. *N*-Acetylcysteine **33** (0.163 g, 1 mmol) and **36** (0.162 g, 1 mmol) were dissolved in 4 mL of DMF and heated at 70 °C for 4 h. The reaction mixture was evaporated to dryness and chromatographed to give **35** as a white solid (0.23 g, 71% yield); mp 118 −119 °C. ^{1}H NMR (in $CDCl_3$): δ 7.32 (m, 5 H), 6.42 (b, $J = 4.5$ Hz, 1 H), 5.88 (b, 1 H), 4.74 (td, $J = 8.8$, 4.5 Hz, 1 H), 4.25 (m, 2 H), 3.58 (s, 2 H), 3.50 (m, 2 H), 2.90 (t d, $J = 8.8$, 4.6 Hz, 2 H); 2.05 (s, 3 H), 1.34 (t, $J = 8.7$ Hz, 1 H). ^{13}C NMR: δ 171.4, 170.2, 170.0, 134.6, 129.5, 129.0, 127.5, 64.6, 53.8, 43.7, 38.5, 26.5, 23.1. HRMS (FAB): *m*/*z* calcd for $C_{15}H_{20}N_2O_4S$ + H, 325.1222; found, 325.1223.

Results and Discussion

Kinetics and Acid Catalysis. As can be seen in Figure 1, the decomposition of *N*-nitrosotolazoline **2** is acid catalyzed by $HClO_4$. At 30 °C in phosphate buffer, the half-lives of **2** range from 5 min at pH 3.5 to 4 h at pH 6 (data not shown). Rate

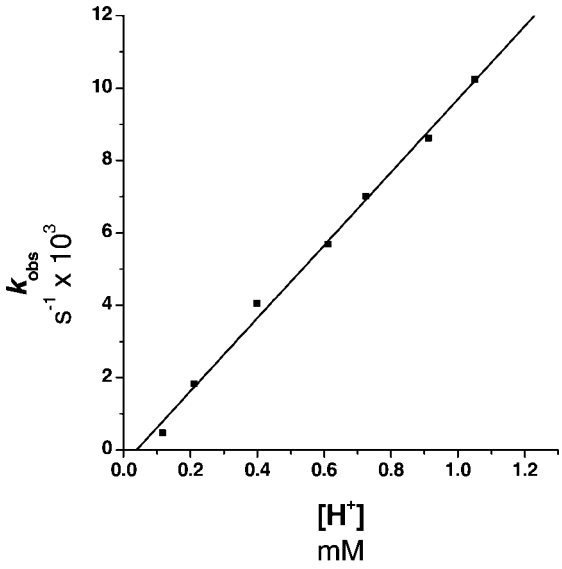

Figure 1. Observed rate constants for the decomposition of *N*-nitrosotolazoline in $HClO_4$ containing 1.0 M $NaClO_4$ at 37.1 °C are plotted against $[H^+]$. The slope as determined by linear regression gives $k_H = 10.1 \pm 0.3\ s^{-1}\ M^{-1}$.

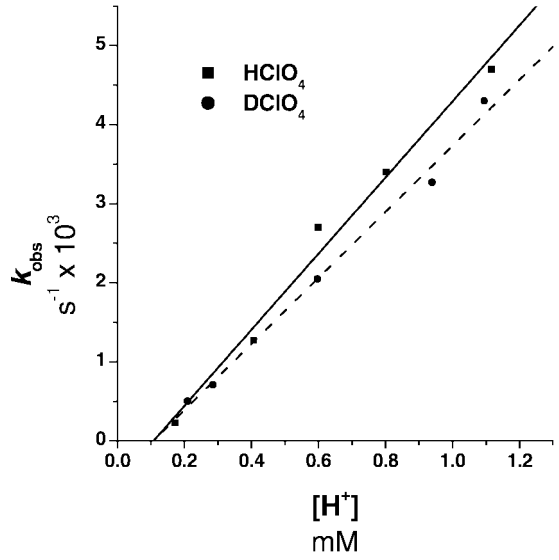

Figure 2. Observed rate constants for the decomposition of *N*-nitrosotolazoline in either $HClO_4$ or $DClO_4$ containing 1.0 M $NaClO_4$ at 25 °C are plotted against $[H^+]$. The slopes were used to calculate $k_H/k_D = 1.15 \pm 0.15$.

constants, the average of at least two determinations, were determined by following the transformation spectrophotometrically and plotting the ln of the absorbance change vs time. Isosbestic points were observed. As can be seen from Figure 1, the rate constants increase linearly with $[H^+]$ in $HClO_4$ at 37 °C giving k_H (the slope of the plot) $= 10.1 \pm 0.3\ s^{-1}\ M^{-1}$. As shown in Figure 2, experiments in $DClO_4$ and its protio counterpart revealed that this acid catalysis is subject to only a modest to insignificant deuterium isotope effect ($k_H/k_D = 1.15 \pm 0.15$), the meaning of which is discussed below. The activation parameters for the decomposition of *N*-nitrosotolazoline in $HClO_4$ (0.73 mM **2**, 1 M $NaClO_4$) were determined by means of rate measurements over a modest temperature range. A plot (Figure 3) of ln (k/T) vs $1/T$ gave a slope and intercept from which $\Delta H^{\ddagger}$ (10.77 ± 0.8 kcal/mol) and $\Delta S^{\ddagger}$ [−33.8 ± 2.5 cal/mol/deg (eu)] could be calculated.

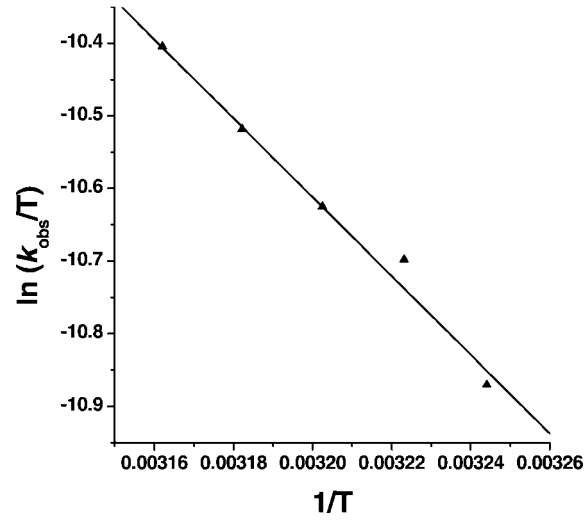

Figure 3. Plot of k_{obs}/T vs $1/T$ (K) over the temperature range 35–43 °C to obtain the $\Delta H^{\ddagger}$ and $\Delta S^{\ddagger}$ is shown.

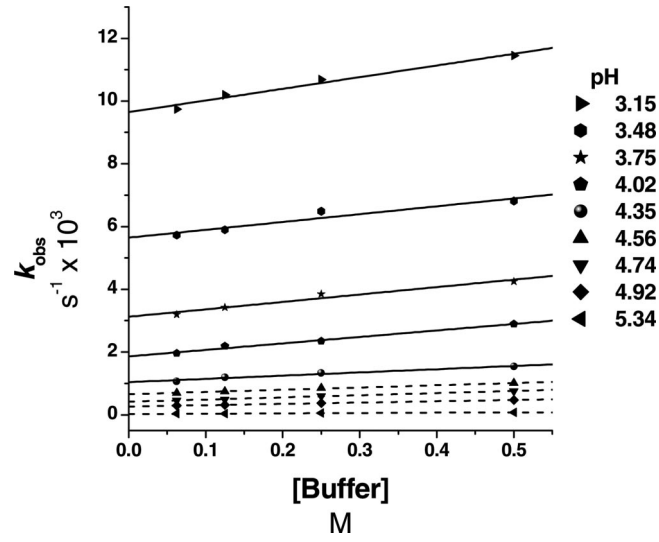

Figure 4. Observed rate constants for the decomposition of *N*-nitrosotolazoline in either formic acid (solid lines) or acetic acid (dashed lines) buffers containing 1.0 M $NaClO_4$ at 37.1 °C are plotted against [buffer]. The slopes and intercepts were used to determine k_{HA} and k_H, respectively, as described.

We also determined reaction rates in acetate and formate buffers at 37 °C over a pH range of 3–6 to further explore the mechanistic details of the transformation. The data are presented graphically in Figure 4. Plots and linear regression of k_{obs} vs [total buffer] at each pH gave the slopes (k_A) listed in Table 1. The values of k_A so determined were then plotted against f_{HA} $\{f_{HA} = [H^+]/(K_A + [H^+])\}$ from which k_{HA} can be determined at $f_{HA} = 1$ for each buffer. The intercepts of the k_{obs} vs [total buffer] plots were, in turn, plotted against $[H^+]$ to give slopes $= k_H$. These data analyses show that there is buffer catalysis and that the transformation is subject to some form of general acid catalysis. While the buffer catalysis is somewhat modest and could be attributed to media effects, we carefully controlled the ionic strength. Accepting the buffer catalysis as a valid experimental observation, we can express k_{obs} as shown in eq 1, where B_T is the [total buffer] and k_w (in formic acid buffer, $0.8 \pm 0.3 \times 10^{-3}\ s^{-1}$; in acetic acid buffer, $0.0 \pm 0.3 \times 10^{-3}$) is the rate constant for H_2O. The zero intercepts of the k_A vs f_{HA} plots represent base catalysis and are not significant for either acid (formic, $0.4 \pm 0.4 \times 10^{-3}\ s^{-1}\ M^{-1}$; acetic, $-0.2 \pm 0.1 \times$

Table 1

pH	$s^{-1}\ M^{-1} \times 10^{-3}$ k_A[a]	error
	formic acid	
3.15	3.72	0.41
3.48	2.50	0.53
3.75	2.37	0.34
4.02	2.06	0.16
4.35	1.03	0.12
k_{HA}[b]	4.3	0.70
k_H[c]	12930	825
	acetic acid	
4.56	0.71	0.039
4.74	0.69	0.046
4.92	0.42	0.011
5.34	0.098	0.003
k_{HA}[b]	1.41	0.25
k_H[c]	27210	1130

[a] Determined from the slopes of linear regression of k_{obs} at each pH vs [total buffer]. [b] Determined from the linear regression equation of k_a vs f_{HA} $\{[H^+]/(K_A + [H^+])\}$ at $f_{HA} = 1$. [c] Determined from the slope of linear regression of intercepts of regression of footnote *a* vs $[H^+]$.

Scheme 1

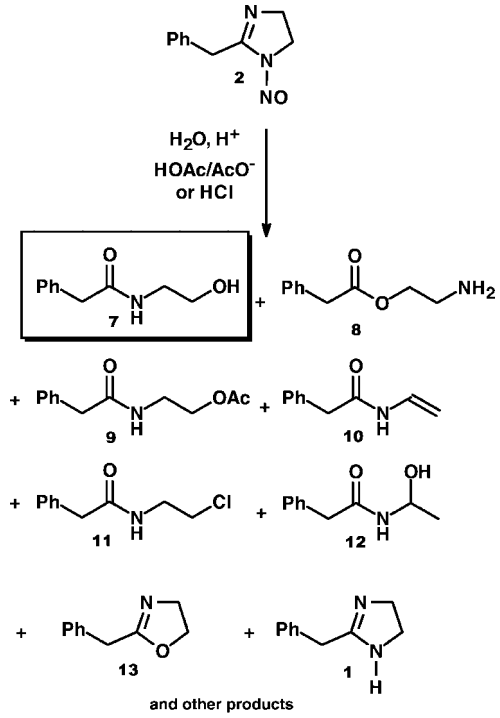

10^{-3} s^{-1} M^{-1}). The mechanistic significance of these data is discussed below.

$$k_{obs} = k_H[H^+] + k_{HA}f_{HA}B_T + K_w \quad (1)$$

Decomposition Products. *N*-Nitrosotolazoline was allowed to decompose in 0.1 M HCl at room temperature, and the resulting aqueous mixture was analyzed by HPLC and extracted with CH_2Cl_2 to isolate the products. HPLC chromatograms of decomposition mixtures produced in $HClO_4$, HCl, and phosphoric acid or acetic acid buffer solutions were also compared. Flash chromatography of the CH_2Cl_2 extract led to the isolation and characterization of products **7**, **10**, and **12**, but not **8** (see Scheme 1). *N*-2-Hydroxyethylphenylacetamide **7** is the major product in all cases and was isolated in 70% yield from the $HClO_4$-catalyzed reaction. A comparison of the HPLC chromatograms of the CH_2Cl_2 extract and the original reaction mixture showed that **8** was not extracted into CH_2Cl_2. Basification of the aqueous extract of the decomposition mixture and extraction with CH_2Cl_2 gave **7**, not **8** (by HPLC). In a separate experiment, the acidic decomposition mixture (0.01 M HCl) was extracted with ethyl acetate and the aqueous mixture was concentrated under high vacuum. Trituration with acetone produced a white solid (**8** as the hydrochloride salt), which cochromatographed with **8** in the acidic reaction mixture. Basification of this salt even at pH 8 led to its conversion to **7** by *O*- to *N*-acyl migration, most likely through an intramolecular rearrangement.

Scheme 2

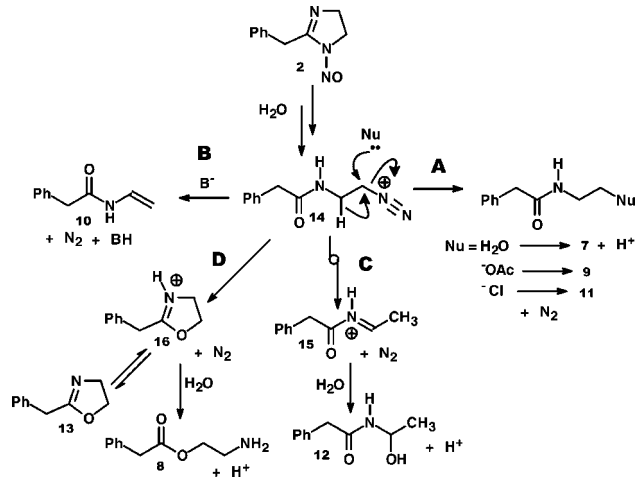

Compounds **7**−**9**, **11**, and **13** are all known compounds and were identified and characterized in our laboratory by ^1H and ^{13}C NMR, IR, and MS spectroscopic methods in comparison with the authentic materials that we prepared. The independent synthesis and characterization of the *N*-vinyl amide **10** have been published (*7*) since the inception of our work. Our ^1H and ^{13}C NMR spectra are identical to those published for this compound. The structure of the amide-hemiaminal, **12**, was initially deduced on the basis of its NMR and IR data, all of which are completely consistent with its assigned structure. However, because we anticipated that such a compound might not survive our reaction and isolation procedures, we confirmed our assignment by X-ray crystallography (see the Supporting Information).

The relative yields of the products vary somewhat depending upon the composition of the acid mixture. In additon to the experiments in perchloric acid and phosphate buffer, we made HPLC comparisons of the product profile from reactions in 0.0012−0.12 M HCl and 0.12 M HOAc. The yields of **7** and **8** decrease in comparison with other products, some of which were not identified, when the hydrolytic decomposition is carried out in acids with more nucleophilic or basic anions, but the differences between the HCl and the HOAc decomposition mixtures were small. In addition to **7**, the yields of which are always >50%, the other major products are **8** (8–10%), **10** (3–5%), **12** (5–6%), and unreacted *N*-nitrosotolazoline (5–6%). In acetic acid, the acetate ester **9** formed in 5%, but the yield of chloride **11** rarely exceeded 3% in the HCl-mediated reactions. Regardless of the acid, the denitrosation product tolazoline **1** yield stayed at about 2%. 2-Benzyl-1,3-oxazoline (*10*) **13** was only a trace component of the mixture with yields <0.7%.

The nature of the products, the relatively large number of minor products, and prior work all permit the reasonable conclusion that all of the products except tolazoline can be rationalized as arising from the diazonium ion **14** (Scheme 2).

Table 2. Comparison of Product Yields from the Hydrolysis of 2 and 13[a]

substrate	*N*-nitrosotolazoline[b] **2**			2-benzyl-1,3-oxazoline[c] **13**		
product/pH	3.5	4.5	5.5	3.5	4.5	5.5
7	69%	71%	70%	1.8%	1.8%	2.2%
8	23%	20%	17%	95%	95%	95%

[a] All hydrolyses were conducted in 0.5 M phosphate buffer at 37 °C. [b] The initial concentration of **2** was 4 mM. [c] The initial concentration of **13** was 4.3 mM.

Scheme 3

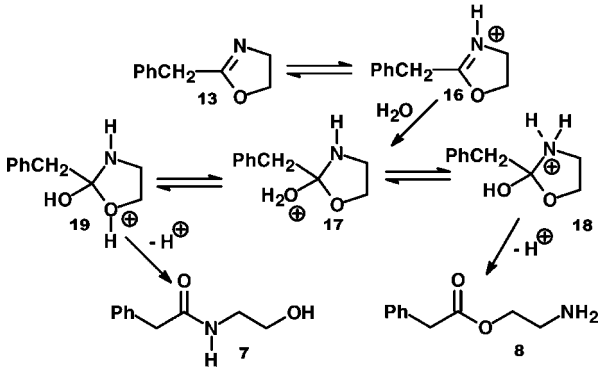

Primary diazonium ions decompose rapidly by SN2 substitution, elimination, and rearrangement pathways. Nucleophilic attack of H_2O on **14** (Scheme 2) gives the major product **7** (path A). Iley et al. (*6*) reported that *N*-nitrotolazoline hydrolyzes in strong acid to produce **7**, which they envisioned to arise through the displacement of N_2O from an intermediate like **14**. The acetate **9** and chloride **11** are produced by similar nucleophilic displacements. Elimination by path B gives **10**. Rearrangement by hydride migration as nitrogen departs gives the resonance-stabilized carbocation **15**, which then gives **12** by attack of H_2O as depicted in path C (Scheme 2). Intramolecular attack of the carbonyl oxygen atom on the diazonium ion carbon gives **16** and then **13** by deprotonation, but this compound is formed in less than 1% from *N*-nitrosotolazoline. In contrast, Iley et al. found that 2-phenyloxazoline and the denitrosation product 2-phenyimidazoline were the major hydrolytic decomposition products of *N*-nitroso-2-phenylimidazoline (*5*). These authors proposed that the oxazoline formed by a pathway identical to path D of Scheme 2. The amino ester **8** can be rationalized to form from the hydrolysis of the protonated oxazoline **16** (Scheme 2); yet, this pathway (D) is not a major competitor to path A in our system. Below, we discuss another possible route to **8**.

In phosphate buffer, the hydrolytic decomposition of *N*-nitrosotolazoline gives only two significant products, **7** and **8** (see Table 2 for yields). If the major pathway involves the intramolecular nucleophilic displacement of N_2 from **14** (path D, Scheme 2), it is possible that **7** as well as **8** arise from the hydrolysis of the oxazoline **13** as shown in Scheme 3 rather than by path A (Scheme 2). The distinction between these pathways has toxicological significance because the intramolecular trapping (path D, Scheme 2) can be viewed as the disarming of a potent electrophile. Intramolecular displacement of N_2 from diazonium ions derived from some cyclic nitrosamines is well-documented (*11–17*), but these transformations yield cations (related to hemiacetals) that can covalently bind DNA in contrast to the formation of the stable oxazoline **13** being considered here. To clarify this point, we prepared 2-benzyloxazoline **13** and compared both its rate of hydrolysis in acid and its hydrolysis products with those arising from *N*-nitrosotolazoline. The $t_{1/2}$ for the hydrolysis of **13** at pH 5.5 is 10 min and is 4.5× faster than that of **2** under the same conditions. Thus, rate studies do not rule out the formation of **7** through the hydrolysis of the oxazoline **13** in the hydrolytic decomposition of **2**, but the product studies do (see Scheme 3). The hydrolysis of **13** gives only minor amounts of **7** (Table 2), whereas **7** is the major product from **2**. In phosphate buffer, 17−23% of the diazonium ion **14** undergoes intramolecular trapping by path D (Scheme 2) as estimated from the yield of **8**. However, the yields of **8** are much lower when the decomposition occurs in HOAc, HCl, or $HClO_4$.

The protonated oxazoline **16** (Scheme 3) will be attacked at the C-2 to generate a tetrahedral intermediate **17**, which is in equilibrium with at least two other forms, **18** and **19**. Additional protonation states for these intermediates could affect the outcome, but the important fact is that **8** is the major hydrolysis product by far. The outcome cannot be easily rationalized of the basis of leaving group ability, NH_2^+ from **18** or one of its conjugate bases vs OH^+ from **19** (or a conjugate base), because the latter is a far better leaving group. On the other hand, because of the basicity of the nitrogen atom, **18** will be the most populated of three tetrahedral intermediates (**17**–**19**) shown. Thus, equilibria could drive the process toward the formation of **8**, as is observed. Consideration of the chemistry depicted in Scheme 3 also gives us a frame of reference for understanding why the hydrolytic decomposition of *N*-nitroso-2-phenylimidazoline results in the isolation of the oxazoline, but the hydrolysis of *N*-nitrosotolazoline does not. 2-Benzyloxazoline **13** must hydrolyze much more rapidly than 2-phenyloxazoline. This is likely due to the conjugative stabilization of the protonated 2-phenyloxazoline by the aromatic ring adjacent to the iminium ion. Thus, either the nucleophilic attack of H_2O to form the requisite tetrahedral intermediate is slower or its equilibrium concentration is lower than what is produced from **16**.

Mechanism of Diazonium Ion Formation. Our kinetic data and literature precedent allow conclusions to be made regarding the hydrolytic decomposition mechanism of *N*-nitrosotolazoline. It is useful to compare our data with those of Iley et al. (*5, 6*) and consider their mechanistic conclusions. The comparisons are summarized in Table 3. In the case of **3**, k_H/k_D is near what is expected for a transformation that proceeds with equilibrium protonation followed by slow, unassisted attack of H_2O to form a tetrahedral intermediate, which decomposes rapidly. Thus, the isotope effect, the specific acid catalysis, and the negative entropy of activation were cited by Iley et al. (*5*) to support their mechanistic conclusion. The observation of curved plots of k_{obs} vs $[H^+]$ for the hydrolytic decomposition of **6** permitted a separation of k_H/k_D for the first two steps (*6*). The nitro substituent markedly decreases the basicity of **6**, and the observation of $k_H/k_D = 0.3$ is consistent with its equilibrium protonation. The conjugate acid so formed was judged to rapidly react with H_2O to generate a tetrahedral intermediate, which is perceived to decompose by a slow cyclic intramolecular transfer of the OH proton to the nitroso O atom with a $k_H/k_D = 1.7$. This conclusion was necessitated by the lack of general acid catalysis and the observation of the large negative entropy of activation associated with a very ordered transition state. This conclusion is also reasonable from a structure−electronic perspective. Because of the powerful electron-withdrawing characteristics of the *N*-nitro group, the 2-carbon of the conjugate acid of **6** should be very susceptible to nucleophilic attack by H_2O, although little of the conjugate acid will be present at modest acidities.

We propose that *N*-nitrosotolazoline is undergoing hydrolytic decomposition to a diazonium ion by the mechanism depicted

Table 3. Comparison of Key Data and Acid Catalyzed Decomposition Mechanisms for 2, 3, and 6

Substrate	k_H/k_D	$\Delta H^{\ddagger}$ (kcal/mol)	$\Delta S^{\ddagger}$ (eu)	Catalysis	Mech. Conclusions
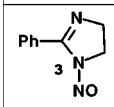	0.29	17	-10	Specific Acid	Rapid equil. protonation, followed by slow attack of H_2O to generate tetrahedral intermediate, which decomposes rapidly.
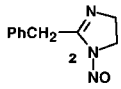	1.15	10.8	-33	General Acid Catalysis: Formate: k_{HA} =4.3 x 10^{-3}; k_H = 12,930 x 10^{-3} Acetate: k_{HA} =1.4 x 10^{-3}; k_H = 27,210 x 10^{-3}	Rapid equil. protonation, followed by general base assisted slow attack of H_2O at C-2 to generate tetrahedral intermediate, which decomposes rapidly.
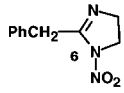	.3 (Eq) 1.7 k_2	14.6	- 23.9	Biphasic (Specific Acid); no Buffer catalysis	Equil protonation followed by reversible attack of H_2O then cyclic decomposition of tetrahedral intermediate with intramolecular proton transfer

Scheme 4

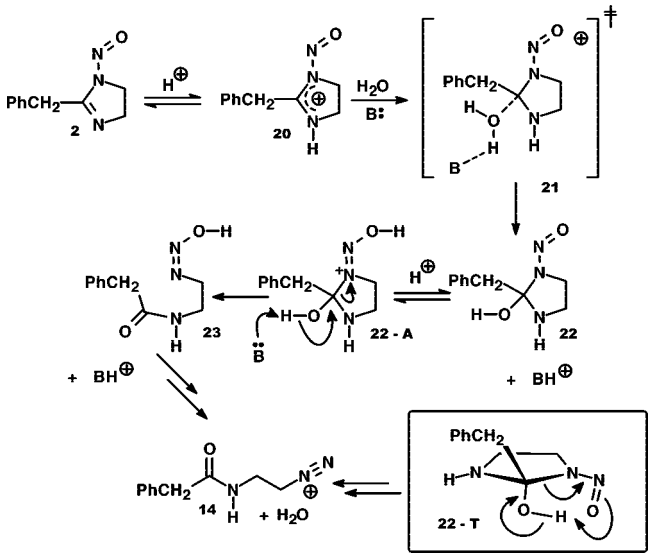

in Scheme 4 where the transition state for the rate-determining step is shown as **21**. This pathway accounts for three notable experimental observations: general acid catalysis, a very modest to insignificant solvent kinetic deuterium isotope effect (SKIE), and the very large negative value of $\Delta S^{\ddagger}$. *N*-Nitrosotolazoline **2** is certainly much less basic than tolazoline but more basic than **3** because the electron-donating benzylic alkyl group at the 2-position enhances basicity as compared to the phenyl group of **3**. *N*-Nitrotolazoline **6** may be less basic than **2**, but this assessment is difficult because both the NO and the NO_2 groups are powerful electron-withdrawing moieties. Like **3**, it is probable that **2** undergoes reversible protonation to **20** (Scheme 4). This step should exhibit a $k_H/k_D \approx 0.3$ because D_3O^+ can be viewed as a stronger acid than H_3O^+ (*18*). Yet, we observe no such SKIE. Conversely, if the protonation of **2** were rate determining, then the SKIE should be ≈3. The observed modest SKIE (1.15) must result from the product of at least two different k_H/k_D values. This could be the case if the attack of H_2O on **20** to give the uncharged tetrahedral intermediate **22** is assisted as shown in **21** by proton transfer from the attacking water molecule to the general base B. The modest nature of the buffer catalysis shows that some, but minor, base assistance occurs in the attack of the H_2O molecule on the cation **20**. Ample literature precedent shows that this step will have a k_H/k_D value of 3 or greater (*18*). Overall, the reaction is specific acid−general base-catalyzed, which is kinetically equivalent to general acid catalysis. This association mechanism involves the loss of a number of degrees of freedom and will have a large negative $\Delta S^{\ddagger}$ (−34 eu), as is observed.

In addition to being a tetrahedral intermediate, so familiar in carbonyl group transformations, **22** is also an α-hydroxynitrosamine. Fishbein et al. (*17, 19, 20*) have carefully studied the catalytic decomposition of these unstable intermediates, which are also the immediate primary metabolic products of nitrosamine carcinogens. The facile decomposition of α-hydroxynitrosamines is subject to acid and base catalysis. 2-Hydroxy-*N*-nitrosopyrrolidine has a $t_{1/2}$ of only 0.03 s at pH 7. General acid-catalyzed hydrolysis is observed in the acid region. Careful analysis of the experimental data led the Fishbein group to conclude that the transformation occurred by equilibrium protonation of the *N*-nitroso O-atom followed by general base-assisted transfer of the α-hydroxy H -atom in the slow step to generate a diazotic acid and an aldehyde (*17, 19, 20*). We show this path in Scheme 4 for the conversion of **22** to **23** through **22-**A. Although we cannot be certain, we believe that this step, regardless of whether it proceeds as depicted or by specific acid−general base catalysis, will not have a large negative $\Delta S^{\ddagger}$. The opening of the ring involves an increase in the degrees of freedom. Transformation through the cyclic transition state shown (**22-**T) may be associated with a significant negative $\Delta S^{\ddagger}$, but this process will not exhibit general acid catalysis. Thus, for our system, we believe that the data best support specific acid−general base formation of **22** in the rate-determining step followed by its rapid decomposition to the reactive diazonium ion **14** as shown or by one of the similar pathways just discussed.

Scheme 5

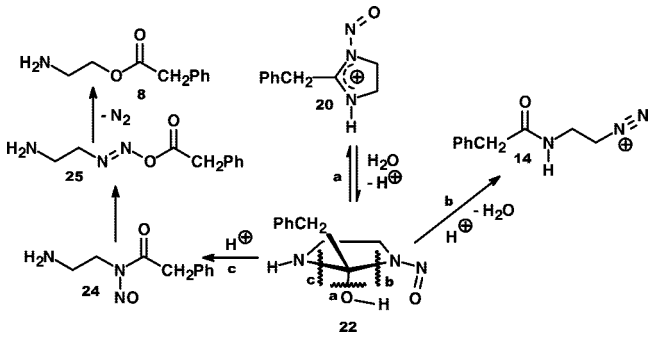

Scheme 6

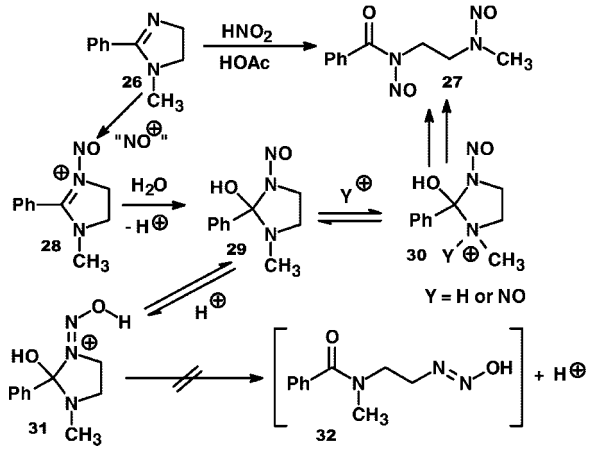

The α-hydroxynitrosamine tetrahedral intermediate **22** can, in theory, decompose by three competing paths, a, b, or c, through acid catalysis as shown in Scheme 5. These paths basically differ in the nature of the leaving group, which we assume to be derived from a protonated intermediate: Path a, H_2O; path b, O-protonated $R_2NN{=}O$; and path c, RNH_2. Path a converts **22** back to the conjugate acid of *N*-nitrosotolazoline. In the case of imidazoline hydrolysis, this is the preferred path as the equilibrium lies on the side of the imidazoline. The cleavage of the other C−N bond (path c) will give the *N*-nitrosoamide **24**. As discussed above, we do find **8**, which is expected to be one of the decomposition products of **24** through **25**, but if this pathway were operative, we would expect to isolate **24** and the other decomposition products produced from it, particularly phenylacetic acid. We previously reported that the nitrosation of 1-methyl-2-phenylimidazoline **26** gives the *N*-nitrosoamide **27** as shown in Scheme 6 (*3*). This work shows that *N*-nitrosoamides akin to **24** can be isolated from acidic nitrosating media. The conversion of **26** to **27** is logically envisioned to occur through the α-hydroxynitrosamine tetrahedral intermediate **29** (Scheme 6), which is similar to **22** (Schemes 4 and 5). In our prior interpretation (*3*), we proposed that the transformation occurs through reversible protonation of **29** to give **30** (Y = H, Scheme 6) that then decomposes as shown by transformations akin to path c of Scheme 5 to give **27**. We did not consider the possible generation of **30**, Y = NO. Although the conditions are different for the hydrolysis of **2** as compared to the acidic nitrosation of **26**, it would superficially appear that **22** (in acid) and **29** (in acid plus nitrous acid) behave differently with respect to acid-catalyzed decomposition, **22** taking path b and **29** proceeding by cleavage of the other C−N bond (c). While this may be the case, our more recent work on amidine (*2*), and particularly tolazoline nitrosation (*1*), show that we must also consider that a second *N*-nitrosation may determine the reaction course, which we now think more probable. The *N*-nitrosation of the $N{-}CH_3$ moiety (**30**, Y = NO) will convert it into a much better leaving group, the incipient nitrosamine, than the protonated amine group (**30**, Y = H). This could determine the course of the reaction as shown. (The $RNNO^-$ anion has been shown to be a poor leaving group (*21*), but we expect the RCH_3NNO^+ group of **30** (Y = NO) to be a good leaving group based on the thermodynamic stability of the incipient nitrosamine functional group.)

The partitioning of an intermediate akin to **22** (Scheme 5) or **29** (Scheme 6) with respect to decomposition paths b and c has been the subject of a recent computational study (*22*). The α-hydroxynitrosamine tetrahedral intermediates (various conformations and nitrosamine stereoisomers) were presumed to arise through the nitrosation of imidazoline itself by a process similar to that shown for the formation of **29** in Scheme 6. The computations showed, of the two pathways considered (not strictly b or c above), that the outcome was determined by the stereochemistry of the N−N=O group in the α-hydroxynitrosamine tetrahedral intermediate akin to **22** or **29**. The retro-ene decomposition route (**22**-T of Scheme 4) is the lowest energy path ($\Delta G^{\ddagger}$ = 12.1 kcal/mol) and is only accessible to the stereoisomer where the N−N=O group is syn to the OH. The syn−anti interconversion barrier between the α-hydroxynitrosamines is large ($\Delta G^{\ddagger} \approx$ 19 kcal/mol in either direction) as compared to the energetics of the retro-ene reaction. Conversion of the α-hydroxynitrosamine tetrahedral intermediate to the *N*-nitrosoamide by C−N cleavage (bond c) was energetically not feasible in the gas phase but did become within reach when the "microsolvation" provided by one H_2O molecule located between the OH and the N of the amine bond being broken was included in the transition state. The activation energy for the conversion of the anti α-hydroxynitrosamine to the *N*-nitrosoamide by this pathway was computed to have a $\Delta G^{\ddagger}$ = 17.3 kcal/mol, which is only 1.9 kcal/mol lower in energy than the syn-anti isomerization barrier. Although there would be some "leakage" across the syn-anti isomerization barrier, the anti α-hydroxynitrosamine was predicted to give rise to the *N*-nitrosoamide to the extent of 95% at 298 K. The activation energy ($\Delta G^{\ddagger}$) for the similar conversion of the syn α-hydroxynitrosamine to *N*-nitrosoamide was computed to be slightly more favorable (16.5 kcal/mol) but large as compared to the retro-ene cleavage of this isomer.

Although we do not know the stereochemistry of *N*-nitrosotolazoline with certainty because only one isomer is present, it is likely the anti (*E*) isomer. The N−N=O stereochemistry of nitrosamines is principally determined by steric factors and the NO group should prefer to be anti to the benzyl group of tolazoline. Assuming that this stereochemical relationship is retained during the addition of H_2O across the C=N, then the anti α-hydroxynitrosamine should be formed and a superficial extension of computational results would appear to predict the formation of the *N*-nitrosoamide **24** as the major product of the hydrolytic decomposition of **2**. We do not observe this outcome. There are several probable explanations for the difference. The protonation of *N*-nitrosotolazoline produces the same intermediate **20** that arises from the nitrosation of tolazoline. The computational modeling of the nitrosation of imidazoline, referred to above, yields a $K = [Z]/[E] \approx 0.01$ and a kinetic barrier of $\Delta G^{\ddagger} < 10$ kcal/mol, giving rise to a very rapid interconversion at 25 °C (see Scheme 7). In the case of **20**, K = [**20**-*Z*]/[**20**-*E*] is likely 0.001 or less, but the barrier is probably not much different. Because the syn-anti (*E*−*Z*) interconversion is rapid as compared to the additon of H_2O to

Scheme 7

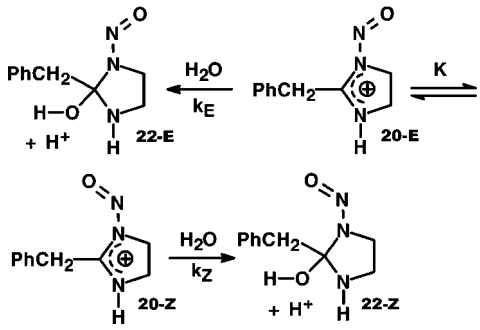

generate the α-hydroxynitrosamines **22-***E* and **22-***Z*, application of the Curtin−Hammett principle shows that the preference for **22-***Z* is given by Kk_Z/k_E. Thus, if $K = 0.001$, then k_Z must be $1000 \times k_E$ to achieve a 1:1 mix of the two stereoisomeric α-hydroxynitrosamines. In other words, $\Delta G^{\ddagger}$ for the generation of **22-***Z* at 25 °C would have to be 4 kcal/mol less than that for the formation of **22-***E* from **20-***E*. The computational study did not calculate transition state energies for the H_2O addition reaction, so we have no computational model against which this argument can be tested. While k_Z may be less than k_E because of the repulsive effect of the lone electron pair on the nitroso N, the experimental work of the Fishbein group (*17, 19, 20*) provides us with a more probable explanation for the differences between our experimental observations and the computational predictions.

As discussed above, the Fishbein group has observed general acid catalysis for all of the α-hydroxynitrosamine decompositions that they have investigated, which includes cyclic and acyclic substrates (*17, 19, 20*). As shown in Scheme 4, they have interpreted this to involve specific acid−general base catalysis. The retro-ene process depicted in **22-**T of Scheme 4, which was assigned by the computation study (*22*) as the decomposition pathway of the syn (*Z*) isomer, is not subject to acid or base catalysis. Therefore, the catalyzed Fishbein pathway **22-***Z* must have a lower $\Delta G^{\ddagger}$ than the retro-ene process, else acid/base catalysis would not be observed. It is also likely that the anti or *E* isomer also decomposes by the Fishbein pathway. These pathways were not subjected to computational modeling (*22*). Thus, while it is possible that *N*-nitrosoamide formation does compete with the Fishbein pathway (*17, 19, 20*), we believe that **8** mainly arises in our decomposition mixture as shown in Scheme 3. This pathway has precedent in the work of Iley et al. (*5*), and we observe little to no phenylacetic acid, a coproduct expected if **24** forms and decomposes. Still, the fact that the nitrosation of **26** only gives the *N*-nitrosoamide **27** (Scheme 6), a process predicted by the computational work so far, shows that subtle factors easily change the chemistry of this system.

Nitrosation of *N*-Nitrosotolazoline. As discussed in the previous paper (*1*), we were unable to isolate significant quantities of *N*-nitrosotolazoline **2** from the nitrosation of tolazoline. The tolazoline nitrosation products were consistent with their actually being products of the nitrosation of *N*-nitrosotolazoline. Our preparative route to **2** involves its continuous CH_2Cl_2 extraction from the nitrous acid solution. Affirmation of our hypothesis that **2** nitrosates much more rapidly than tolazoline **1** was aided by our finding that the amide **7** is the main product from the acid-catalyzed decomposition of **2** but is not produced from the nitrosation of **1**. The amide **7** is stable toward our nitrosation conditions. Although we found it difficult to compare the respective nitrosation kinetics of **1** and **2**, we estimated on the basis of half-lives, under the stated conditions of each transformation, that **2** nitrosates at least 50×

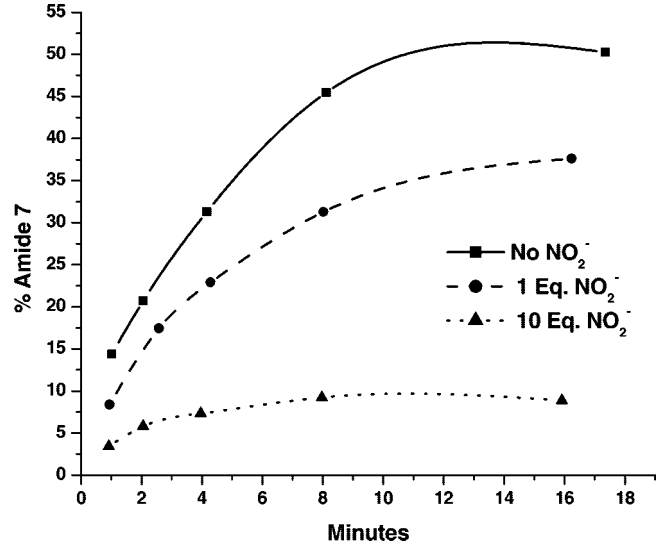

Figure 5. Yields of *N*-2-hydroxyethylphenylacetamide **7** produced from *N*-nitrosotolazoline **2** are compared as a function of reaction conditions in 0.5 M acetate buffer at pH 3.4 at 37 °C. Nitrosation significantly reduces the yield of **7**, the normal hydrolysis product, which is not a nitrosation product.

faster than **1** in buffered HOAc containing 10 equiv of NO_2^- at 37 °C. The % yield of **7** as a function of time can be used to probe the competition between the hydrolysis of **2** and its nitrosation as is shown in Figure 5. Addition of 1 equiv of nitrite to the acidic mixture reduces the final yield of **7** from 50 to 35%, and 10 equiv of NO_2^- limit the final yield of **7** to 9%. The much more facile nitrosation of **2** is undoubtedly due to its much lower basicity than **1**, since it is the free base that is nitrosated.

Reaction of *N*-Acetylcysteine with *N*-Nitrosotolazoline. With the exception of diarylnitrosamines, most nitrosamines do not undergo denitrosation at a measurable rate unless the reaction is carried out in very strong mineral acid (*23, 24*). Under these conditions, halide ions, thiocyanate, and several other sulfur compounds are effective catalysts of this transformation. On the other hand, *N*-nitrosoamides, -ureas, and -urethanes, which have a carbonyl bound adjacent to NNO group, denitrosate with much greater facility (*25, 26*). As discussed above, Iley et al. reported that *N*-nitroso-2-phenylimidazoline denitrosates significantly under the conditions of its acid-catalyzed hydrolysis (*5*). This is not true of **2**, but glutathione and thiol-induced denitrosation transformations can be modulators of the carcinogenicity and toxicity of some *N*-nitroso compounds. For example, *N*-nitrosocimetidine is produced by the gastric nitrosation of the antiulcer drug cimetidine (*27*). However, studies showed that this *N*-nitrosocyanoguanidine was rapidly denitrosated by thiols including those contained in blood-circulating proteins (*27*). On the basis of these observations, we thought it important to perform a preliminary examination of the interaction between **2** and *N*-acetylcysteine **33**.

In phosphate buffer at pH 5, 25 °C, *N*-acetylcysteine **33** diminishes the $t_{1/2}$ of *N*-nitrosotolazoline **2**. As the concentration of **33** is increased from 0 to 0.01, 0.1, and 0.5 M, the respective half-lives (min) of **2** are as follows: 36.5, 33.0, 28.7, and 19.6. A more dramatic change is observed at pH 7 as shown in Figure 6. Under these conditions (pH 7, 25 °C), *N*-nitrosotolazoline in a 0.1 M acetate containing solution (control) has a $t_{1/2}$ of 213 h but only a $t_{1/2}$ of 8.15 h in a 0.1 M solution of **33**. The major decomposition product, even in the presence of 500 mM **33**, is the diazonium ion-derived amide **7** (see Scheme 3). At pH 5, concentrations of **33** below 100 mM have little effect on the

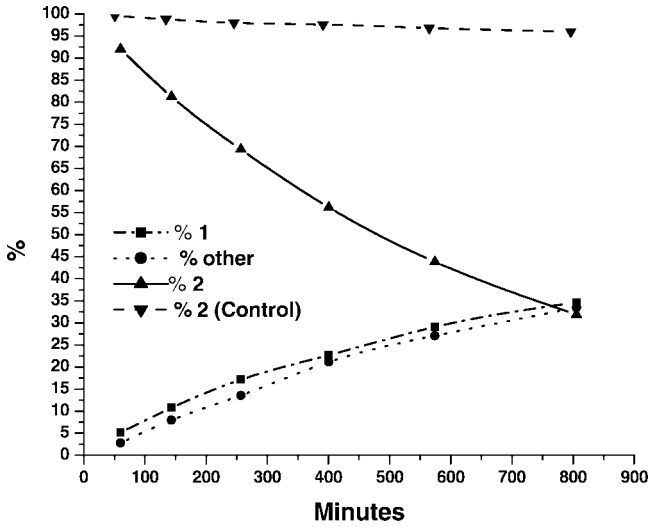

Figure 6. Effect of 0.1 M *N*-acetylcysteine **33** at pH 7 on the concentration of *N*-nitrosotolazoline **2** (initial, 1.8 mM) as a function of time is shown. The control experiment shows the concentration of **2** under the same conditions except that the *N*-acetylcysteine was replaced with sodium acetate. Tolazoline **1**, the denitrosation product, increases as **2** decreases but accounts for slightly greater than 50% of the products derived from **2**. The % of the others, arrived at by adding the concentrations of **1** and **2** and subtracting the sum from 100, increases at the same rate and shows that **33** induces the decomposition of **2**.

Scheme 8

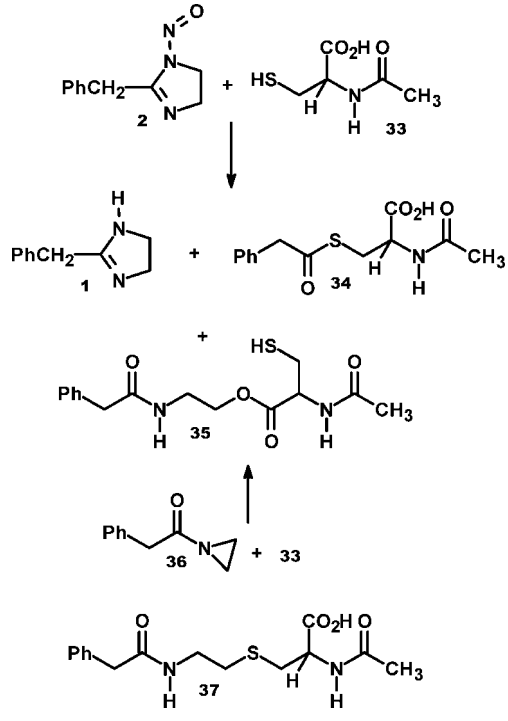

composition of the product mixture. *N*-Acetylcysteine (500 mM, pH 5, 25 °C, 77 min) reduces the yield of **7** from 47 (no **33**) to 36%, while the yield of tolazoline increases from 0 to 13%. A comparison of the HPLC chromatograms of the pH 5 reaction mixtures with those from the acid-catalyzed hydrolysis of **2** showed that the diminished $t_{1/2}$ of **2** was due to appearance of three new reaction products. One of these was the denitrosation product tolazoline **1**. The other two compounds, **34** and **35** (see Scheme 8), were isolated by chromatography and characterized by NMR, MS, and ultimately synthesis. Relative product yields at pH 4 are given in Table 4. The phenylacetyl thio-ester of **33**

Table 4. Relative Product Yields from the Reaction of 2 with 33

compound	relative %[a]
1	21.5
8	5.1
7	38.8
12	4.2
34	20.7
35	4.2
10	1.7
2	3.7

[a] Determined by HPLC from the reaction of **2** (2.47 mM) in the presence of 0.5 M **33** in pH 4 phosphate buffer at 25 °C after 75 min.

(**34**) was synthesized by reaction **33** with phenylacetyl chloride. We anticipated that **33** would scavenge electrophiles produced in the decomposition of **2**, principally the diazonium ion **14**, and expected the sulfide **37** (Scheme 8) to be a product. The NMR spectral properties of compound **35** are inconsistent with it being assigned the structure **37**. Both the ^{1}H and the ^{13}C NMR spectra of the imidazoline-derived fragment exhibit chemical shifts very close to those observed for **7**, which has the same atom connectivity. If the terminal CH_2 were attached to S as in structure **37**, then this carbon and its attached protons would be found at higher field. As it is, the ^{13}C and ^{1}H for this CH_2 are at δ 64.51 and δ 4.25, respectively, positions clearly consistent with a CH_2-O group. This compound also exhibits at triplet at δ 1.34, which we have assigned to the SH. As shown in Scheme 8, **35** was synthesized by the reaction of **33** with *N*-phenylacetylaziridine **36**. Although this is not an unambiguous synthesis, the spectral characteristics of **35** are clearly in accord with its structural assignment.

The data shown in Figure 6 clearly show that **33** induces the decomposition of **2** as compared to the control. The $t_{1/2}$ drops by an estimated factor of 25. The denitrosation product **1** represents only slightly more than 50% of the product mixture under these conditions. The product studies at pH 4 and 5 are also indicative of induced decomposition but, as compared to the controls and the effects, are greater at higher pH, which suggests the involvement of a base-catalyzed process. At pH 4, the yield of **1** is only 21.5% but the yield of **34** is 20.7% (see Table 4). Thus, **33** must be inducing the decomposition of **2** as well as denitrosating it by thiol attack on the NO group. Moreover, the structure of **34** suggests that it has been formed by attack of the thiol group of **33** at the C=N of **2**. Thiol induction of the decomposition and denitrosation of *N*-methyl-*N*′-nitro-*N*-nitrosoguanidine (MNNG) has been reported by several groups. These processes are well-reviewed and cited in the detailed mechanistic work of the Fishbein group (*26*). A possible route, which could involve acid or base catalysis, is shown in Scheme 9 and is broadly consistent with the Fishbein mechanism (*26*), although they did not work in the acidic pH range. A reactive diazonium ion **39** is formed by decomposition of the tetrahedral intermediate **38**. While it can participate in various inter- and intramolecular transformations, the simplest process envisions its hydrolytic conversion to **40**, which then hydrolyzes to give the thioester **34** and ethanolamine **41**, which would escape detection by our analytical method. While **35** can also be rationalized to arrive from **39**, it probably comes from a reaction of the diazonium ion **14** produced by the acid-catalyzed decomposition of **2** with **33**. The thiol is the most nucleophilic moiety in **33**, but it will not be in its more nucleophilic thiolate form at the pH of the product study, while a significant fraction of the carboxyl groups will be present as the carboxylate anions. Carboxylate attack on the diazonium carbon of **14** provides some rationale for the surprising formation

Scheme 9

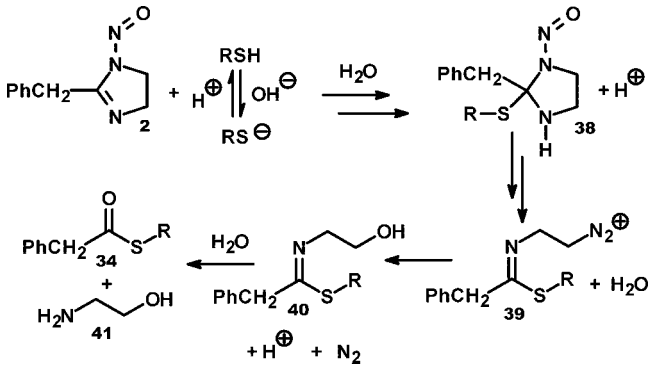

of **35** rather than **37**. There is ample precedent for thiol-induced denitrosation reactions (*28*). Thus, assuming that it is the thiol function, which is responsible for the denitrosation and the induction of decomposition, biological thiols are expected to have profound effect on the fate of **2**.

Conclusion

We have presented details of the chemistry of *N*-nitrosotolazoline **2** under three conditions, which may be relevant to human health: decomposition in acid such as what exists in the stomach, nitrosation under conditions that may form *N*-nitrosotolazoline endogenously (*1*), and *N*-acetylcysteine-induced transformations that could be representative of the reactions of biological thiols with **2** or similar *N*-nitrosoimidazolines. Although tolazoline, from which **2** is derived by nitrosation, is an over-the-counter and prescription drug, the research presented here is likely more significant because the properties of **2** are logically expected to appropriately model the chemistry of other *N*-nitrosoimidazolines. *N*-Nitrosotolazoline nitrosates much more rapidly than its precursor tolazoline. As we have shown, this process directly produces a cascade of electrophiles capable of damaging DNA, proteins, and other important biological nucleophilic molecules.

N-Nitrosotolazoline readily decomposes in acidic solution to generate a highly reactive diazonium ion **14** from which the alcohol **7** is derived. The amino ester **8** is a minor product of this decomposition and is perceived to arise from intramolecular trapping of the diazonium ion followed by the rapid hydrolysis of the derived oxazoline **13**. The extent of this trapping is a function of the catalytic acid, is lowest in mineral acids, and is always <23%. In this way, **2** behaves quite differently than the extensive intramolecular trapping reported for the diazonium ion derived from *N*-nitroso-2-phenylimidazoline **3**. We also observed very little (<2%) denitrosation of **2** under the conditions of its acidic hydrolytic decomposition. The mechanism of the acid-induced decomposition of **2**, as justified by physical chemical parameters and literature precedent, is perceived to involve the rapid reversible protonation of the imino nitrogen atom followed by slow general base-catalyzed addition of H_2O to the 2-carbon to give the resulting α-hydroxynitrosamine **22**, which is also a tetrahedral intermediate. Rapid decomposition of this species gives rise to the diazonium **14** from which the products are derived by nucleophilic attack, elimination, and rearrangement. In the following paper, we show that the electrophiles so produced readily alkylate DNA (*29*).

N-Acetylcysteine increases the decomposition rate of **2** 25-fold at pH 7 and both denitrosates and induces its decomposition to produce electrophiles. These processes occur to comparable extents. Thus, the chemistry of **2**, which we expect to be representative of *N*-nitrosoimidazolines, results in the production of potent cell-damaging electrophiles. Even if these nitroso compounds are not formed in the acidic stomach but, for example, at a site of chronic inflammation where endogenous nitrosation occurs, such as a chronically infected sinus, our chemical data suggest the formation of reactive electrophiles. The chemical properties of *N*-nitrosotolazoline are also characteristic of other mutagenic and carcinogenic *N*-nitroso compounds. On this basis, we conclude that *N*-nitrosoimidazolines are likely direct-acting mutagens and carcinogens.

Acknowledgment. This research was supported by Grant RO1 CA85538 from the National Cancer Institute, NIH. R.N.L. thanks Profs. J. Iley and J. Fishbein for their helpful discussions of acid catalysis. The X-ray structure of **12** was kindly provided by Dr. Charles H. Barnes (University of Missouri).

Supporting Information Available: Selected ^1H and ^{13}C NMR spectra, an Ortep drawing of the X-ray-determined structure for **12**, and crystallographic data for this structure. This material is available free of charge via the Internet at http://pubs.acs.org.

References

(1) Loeppky, R. N., Shi, J., Barnes, C., and Geddam, S. (2008) A diazonium cascade from the nitrosation of tolazoline, an imidazoline containing drug. *Chem. Res. Toxicol. 21*, 295–307.
(2) Loeppky, R. N., and Yu, H. (2004) Amidine nitrosation. *J. Org. Chem. 69*, 3015–3024.
(3) Loeppky, R. N., and Cui, W. (1998) The nitrosation of imidazolines and oxazolines. *Tetrahedron Lett. 39*, 1845–1848.
(4) Loeppky, R. N., and Yu, L. (1990) Nitrosamines, *N*-nitrosoamides, and diazonium ions from tri-*N*-substituted amidines. *Tetrahedron Lett. 31*, 3263–3266.
(5) Iley, J., Norberto, F., and Rosa, E. (1989) *N*-Nitroso compounds. Part 1. Structure and decomposition of *N*-nitroso-2-arylimidazolines in aqueous acidic media. *J. Chem. Soc., Perkin Trans. 2* 1471–1475.
(6) Iley, J., Norberto, F., and Sardinha, P. (1998) The acid-catalysed decomposition of *N*-nitrotolazoline. *J. Chem. Soc., Perkin Trans. 2 1998*, 2207–2209.
(7) Hansen, A. L., and Skrydstrup, T. (2005) Fast and regioselective Heck couplings with *N*-acyl-*N*-vinylamine derivatives. *J. Org. Chem. 70*, 5997–6003.
(8) Behrens, O. K., Corse, J., Jones, R. G., Mann, M. J., Soper, Q. F., Van Abeele, F. R., and Chiang, M.-C. (1948) Biosynthesis of penicillins. I. Biological precursors for benzylpenicillin (pencillin G). *J. Biol. Chem. 175*, 751–764.
(9) Boggs, G. R., and Gerig, J. T. (1969) Nitrogen inversion in *N*-benzoylaziridines. *J. Org. Chem. 34*, 1484–1486.
(10) Partridge, M. W., and Turner, H. A. (1949) Synthesis of 1-aryl-4,5-dihydroglyoxalines. *J. Chem. Soc.* 1308–1310.
(11) Wang, M., Young-Sciame, R., Chung, F.-L., and Hecht, S. (1995) Formation of N^2-tetrahydrofuranyl and N^2-tetrahydropyranyl adducts in the reactions of α-acetoxy-*N*-nitrosopyrrolidine and α-acetoxy-*N*-nitrosopiperidine with DNA. *Chem. Res. Toxicol. 8*, 617–624.
(12) Young-Sciame, R., Wang, M., Chung, F.-L., and Hecht, S. (1995) Reactions of α-acetoxy-*N*-nitrosopyrrolidine and α-acetoxy-*N*-nitrosopiperidine with deoxyguanosine: Formation of N^2-tetrahydrofuranyl and N^2-tetrahydropyranyl adducts. *Chem. Res. Toxicol. 8*, 607–616.
(13) Wang, M., Chung, F. L., and Hecht, S. S. (1989) Formation of acyclic and cyclic guanine adducts in DNA reacted with α-acetoxy-*N*-nitrosopyrrolidine. *Chem. Res. Toxicol. 2*, 423–428.
(14) Chung, F. L., Wang, M., and Hecht, S. S. (1989) Detection of exocyclic guanine adducts in hydrolysates of hepatic DNA of rats treated with *N*-nitrosopyrrolidine and in calf thymus DNA reacted with α-acetoxy-*N*-nitrosopyrrolidine. *Cancer Res. 49*, 2034–2041.
(15) Hecht, S. S., and Chen, C.-H. B. (1979) A study of chemical carcinogenesis. 14. Hydrolysis of model compounds for α-hydroxylation of the carcinogens *N*-nitrosopyrrolidine and *N*′-nitrosonornicotine. *J. Org. Chem. 44*, 1563–1566.
(16) Zink, C. N., Kim, H.-J., and Fishbein, J. C. (2006) Synthesis and aqueous chemistry of α-acetoxy-*N*-nitrosomorpholine: Reactive intermediates and products. *J. Org. Chem. 71*, 202–209.
(17) Kim, H.-J., and Fishbein, J. C. (2003) Reexamination of the aqueous chemistry of *N*-nitroso-3-hydroxymorpholine, a metabolite of the carcinogen *N*-nitrosomorpholine. *Chem. Res. Toxicol. 16*, 715–720.

(18) Jencks, W. P. (1987) *Catalysis in Chemistry and Enzymology*, Dover Publications, Inc., New York.

(19) Mesic, M., Peuralahti, J., Blans, P., and Fishbein, J. C. (2000) Mechanisms of decomposition of α-hydroxydialkylnitrosamines in aqueous solution. *Chem. Res. Toxicol. 13*, 983–992.

(20) Mesic, M., Revis, C., and Fishbein, J. C. (1996) Effects of structure on the reactivity of α-hydroxydialkylnitrosamines in aqueous solutions. *J. Am. Chem. Soc. 118*, 7412–7413.

(21) Wichems, D. N., Nag, S., Mills, J., and Fishbein, J. C. (1992) Evidence for intermediates and a change in rate-limiting step in the aminolysis of the carcinogen *N*-methyl-N′-nitro-*N*-nitrosoguanidine by cyclic amines. *J. Am. Chem. Soc. 114*, 8846–8851.

(22) Wu, H., Loeppky, R. N., and Glaser, R. (2005) Nitrosation chemistry of pyrroline, 2-imidazoline, and 2-oxazoline: Theoretical Curtin-Hammett analysis of retro-ene and solvent-assisted C-X cleavage reactions of α-hydroxy-*N*-nitrosamines. *J. Org. Chem. 70*, 6790–6801.

(23) Williams, D. L. H. (1975) Reaction of a nitrosamine with thiourea. Direct sulfur nitrosation. *J. Chem. Soc., Chem. Commun.* 375–376.

(24) Dix, L. R., Oh, S. M. N. Y. F., and Williams, D. L. H. (1991) Denitrosation of nitrosamines—A quantitative study. Reactions of *N*-methyl-*N*-nitrosoaniline, *N*-nitrosoproline, dimethylnitrosamine and *N*-nitrososarcosine. *J. Chem. Soc., Perkin Trans. 2* 1099–1104.

(25) Williams, D. L. H. (1988) *Nitrosation*, Cambridge University Press, Cambridge, United Kingdom.

(26) Santala, T., and Fishbein, J. C. (1992) Thiolytic decomposition of the carcinogen *N*-methyl-*N*′-nitro-*N*-nitrosoguanidine. A change in rate-limiting step with nucleophile basicity controls alkylating activity. *J. Am. Chem. Soc. 114*, 8852–8857.

(27) Jensen, D. E., and Magee, P. N. (1990) Nitrosation of cimetidine and biological consequences: An overview. In *The Significance of N-Nitrosation of Drugs* (Eisenbrand, G., Bozler, G., and Nicolai, H. v., Eds.) pp 235–250, Gustav Fischer Verlag, Stuttgart.

(28) Williams, D. L. H. (1985) *S*-Nitrosation and the reactions of *S*-nitroso compounds. *Chem. Soc. Rev. 14*, 171–196.

(29) Loeppky, R. N., and Shi, J. (2008) Nucleoside and DNA adducts from *N*-nitrosotolazoline. *Chem. Res. Toxicol. 21*, 319–329.

TX700318K